Thermochimica Acta, 205 (1992) 259–269
Elsevier Science Publishers B.V., Amsterdam

Study by electrical conductivity, derivative thermogravimetry, infrared spectrometry and X-ray photoelectron spectroscopy of oxidation process of Fe_2MoO_4 in relation to the cationic distribution

B. Domenichini and B. Gillot

Laboratoire de Recherche sur la Réactivité des Solides associé au CNRS, UA 23, Faculté des Sciences Mirande, B.P. 138, 21004 Dijon Cedex (France)

P. Tailhades

Laboratoire de Chimie des Matériaux Inorganiques, U.R.A.C.N.R.S. 1311, Université Paul Sabatier, 118, route de Narbonne, 31062 Toulouse Cedex (France)

(Received 1 October 1991)

Abstract

The thermal behaviour in oxygen of Fe_2MoO_4 spinel prepared by the ceramic method has been investigated over the temperature range of 150–700°C on ground samples. Below 550°C, Fe_2MoO_4 is partially oxidized in the cation deficient spinel with a very large content of vacancies. The high electrical conductivity of the initial sample and its temperature dependence in oxygen can be related to a mixture of Fe^{2+} and Fe^{3+} valencies on both octahedral (B) and tetrahedral (A) sites, despite the observed positive value of the Seebeck coefficient. Derivative thermogravimetric studies showed that B site Fe^{2+} and Mo^{3+} ions will be oxidized more rapidly than A site Fe^{2+} ions when the oxidation temperature is lower for Fe^{2+} ions on B sites than that for Mo^{3+} ions on the same sites, and this discrepancy in reactivity has been used to determine the distribution of cations between the sublattices. In addition, a significant content of Mo^{4+} ions and a transfer of Mo^{6+} ions from the B sites to the A sites during oxidation can be derived from XPS and IR spectrometry.

INTRODUCTION

The spinel Fe_2MoO_4 is a mixed-valent oxide. It attracted early attention because its unusually high electrical conductivity (10^{-2} Ω cm^{-1} at room temp.) stands in contrast to the cation distribution previously reported [1–3], $(Fe^{2+})_A(Fe^{2+}Mo^{4+})_BO_4^{2-}$ or $(Fe^{3+})_A(Mo^{3+}Fe^{2+})_BO_4^{2-}$, where the subscripts A and B refer, respectively, to occupancy of tetrahedral or octahedral sites of the spinel structure.

Correspondence to: B. Gillot, Laboratoire de Recherches sur la Réactivité des Solides associé au CNRS, UA 23, Faculté des Sciences Mirande, B.P. 138, 21004 Dijon Cedex, France.

A good electrical conductivity in a spinel is generally associated with a mixed cation valence on energetically equivalent neighbouring lattice sites, as occurs, for example, in ferrites [4,5] and manganites [6], when the maximum of conductivity corresponds to a maximum number of $M^{n+}-M^{(n+1)+}$ ion pairs on B sites. Gupta et al. [7] and, most recently, Ramdani et al. [8] concluded from Mössbauer data and electrical measurements that fast electron exchange takes place amongst Fe^{3+} and Fe^{2+} ions located at B as well as at A sites in the spinel lattice, yielding a possible cation distribution

$$(Fe^{2+}_{0.5}Fe^{3+}_{0.5})_A(Mo^{3+}Fe^{2+}_{0.5}Fe^{3+}_{0.5})_B O^{2-}_4 \qquad (1)$$

The presence of a small amount of Mo^{4+} ions should also be considered [8], and the strong B-site preference of Mo^{3+} and Mo^{4+} ions forces a cation arrangement of the type

$$\left(Fe^{3+}_{\beta}Fe^{2+}_{1-\beta}\right)_A\left(Mo^{3+}_{1-\alpha}Mo^{4+}_{\alpha}Fe^{2+}_{1+\alpha}-\beta Fe^{3+}_{\beta-\alpha}\right)_B O^{2-}_4 \qquad (2)$$

where $\beta = 0.5$ and $\alpha \to 0$.

However, whatever the proposed cation configuration, this spinel contains several oxidizable cations (Fe^{2+}, Mo^{3+}, Mo^{4+}) distributed on both A and B sites of the spinel structure. During a detailed study of the oxidation mechanism of some magnetites substituted by divalent, trivalent or tetravalent ions [9,10] in cation deficient spinels, it was found that the oxidation temperature and the electrical conductivity are related to the cation distribution. The oxidation temperature of B site M^{n+} ions is lower than that of A site M^{n+} ions because of the weaker ionic bonding of the B sites as compared with the stronger A site covalent bond. Moreover, the possible occupation of the B sites by several oxidizable cations (Mo^{3+}, Mo^{4+}, Fe^{2+}) requires a careful consideration of the availability for oxidation of these different cations located in the same sublattice.

In this paper we report the results of our attempts to use the electrical conductivity and derivative thermogravimetry to characterize the process of oxidation of Fe_2MoO_4. These results are compared with the conductivities of polycrystalline Fe_2CrO_4 and Fe_2AlO_4 spinels, which also present oxidizable cations in A and B sites of the spinel structure. Some important clues on the thermal stability in oxygen, cation valency and cationic migration are obtained from the investigation by means of IR spectrometry and X-ray photoelectron spectroscopy (XPS).

EXPERIMENTAL PROCEDURE

The spinel Fe_2MoO_4 was prepared by mixing in an agate mortar powders of Fe, Fe_2O_3 and MoO_2 in the stoichiometric proportion. The well homogenized powder was put into an alumina crucible placed inside a silica ampoule. The ampoule was then degassed under vacuum (10^{-9} Pa) in order to avoid oxidation at high temperature, sealed and heated at 1150°C for 3 h, after which it was quenched. The sample was analysed by X-ray diffraction and was found to have a single phase cubic spinel structure with a lattice parameter of $a = 0.8512$ nm. The methods of preparation of Fe_2CrO_4 and Fe_2AlO_4 from oxalate precursors have been previously indicated [10].

The d.c. conductivity and Seebeck coefficient were measured point by point under a N_2 atmosphere or in oxygen by means of a two-probe device on compressed pellets, as reported in ref. 11. Such an arrangement correctly provides the activation energy; the conductivity values are generally smaller than those obtained with single crystals.

The samples were oxidized in a Setaram MTB 10-8 microbalance with the temperature increasing at a linear rate (2.5°C min^{-1}) or under isothermal conditions. The material weighed 6 mg and the ground powder was spread out so that it would be oxidized in the same way as N independent particles of equal mean radius. Fourier transform infrared (FT-IR spectra) were recorded using a Perkin–Elmer 1725X spectrometer and the CsI discs technique. X-ray photoelectron spectroscopy results were obtained using a Riber AES-ESCA-ELS MA62 instrument equipped with an Al anode, which was operated at 13 kV and 20 mA emission current ($h\nu = 1486.6$ eV). Binding energies were determined using the C1*s* peak at 285 eV and the oxide powder was pressed onto a piece of indium foil (99.999%), which was earthed to the spectrometer during the examination.

RESULTS

Electrical measurements

For a number of polycrystalline Fe_2MoO_4 and Fe_2MO_4 ($M = Cr^{3+}$, Al^{3+}) spinels, Fig. 1 displays under a N_2 atmosphere the variation of $\lg \sigma T$ versus $1/T$. In these three spinels, one change of slope is observed that occurs approximately at the Curie temperature (T_C) but, interestingly, the conductivity of Fe_2MoO_4 is roughly a factor of 10 higher that the conductivities of the other spinels. This high conductivity is associated with a low activation energy for temperatures above T_C (Table 1), indicating that in the paramagnetic state the conduction takes place through hopping of the charge carriers from one site to another. Fe_2CrO_4, with an activation energy of 0.27 eV (Table 1), contains mixed Fe^{2+} and Fe^{3+} valencies on both B and A sites [12,9] according to the distribution $(Fe^{2+}_{0.55}Fe^{3+}_{0.45})_A(Fe^{2+}_{0.45}Fe^{3+}_{0.55}Cr^{3+})_B O_4^{2-}$; the number of charge carriers (Fe^{2+}/Fe^{3+} ratio $= 1$) is large, and hence the activation energy for this type of distribution is low, as for Fe_2MoO_4. In the case of Fe_2AlO_4 with the distribution [10] $(Fe^{2+}_{0.15}Fe^{3+}_{0.85})_A(Fe^{2+}_{0.85}Fe^{3+}_{0.15}Al)_B O_4^{2-}$, the low conductivity and high activation energy (Table 1) can be explained by assuming that with an Fe^{2+}/Fe^{3+}

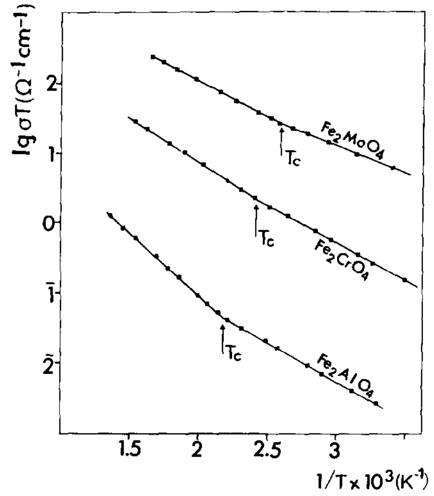

Fig. 1. Temperature dependence of the electrical conductivity σ under N_2 atmosphere plotted as lg σT vs. $1/T$ for MFe_2O_4 (M = Mo, Cr, Al).

ratio > 5 the number of charge carriers is small and hence the activation energy for this type of distribution should be high. The comparable activation energies for Fe_2MoO_4 and Fe_2CrO_4 imply a similar conduction mechanism, i.e. conduction via a mixed Fe^{3+}/Fe^{2+} valence on both A and B sites, which gives rise to mobile small polarons on the B sites. Moreover, the fact that the thermoelectric power θ is nearly temperature independent for $T < 500°C$ is in favour of a mechanism of hopping of electrons between B iron ions [13]. However, the measured value at room temperature (+27 $\mu V\ °C^{-1}$) can only be interpreted if we consider that the mobile electrons have nearly equal access to both A and B sites and to a fraction of the Mo_B atoms [8] when the molybdenum is at least partially oxidized to the Mo^{4+} state.

The effect of temperature on oxidation characteristics was demonstrated directly by observing the plots of lg σ vs. $1/T$ when the samples were heated in air at a constant rate of 1°C min^{-1} from room temperature to 750°C (Fig. 2). For Fe_2MoO_4, the conductivity initially increases, giving a

TABLE 1

Electrical parameters of MFe_2O_4 spinels (M = Mo, Cr, Al) under N_2 atmosphere

Sample	Activation energy (eV)	T_C (K)	θ ambient ($\mu V\ K^{-1}$)
Fe_2MoO_4	0.26	395	+27
Fe_2CrO_2	0.27	407	−35
Fe_2AlO_4	0.37	447	+90

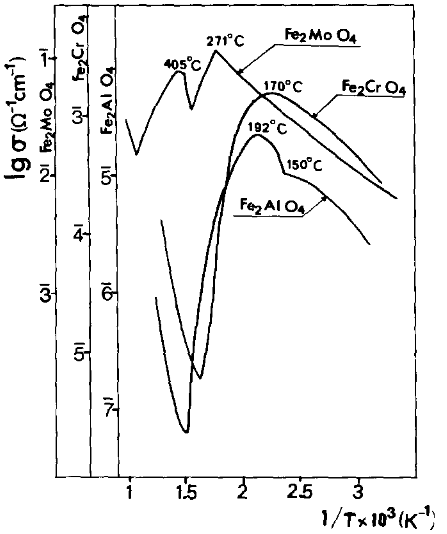

Fig. 2. Behaviour of electrical conductivity for MFe_2O_4 spinels (M = Mo, Cr, Al) heated in air at 1°C min^{-1}.

first maximum at about 271°C. The conductivity then decreases and again increases with a second maximum at 405°C. In comparison, we have also represented the heating curves for Fe_2CrO_4 and Fe_2AlO_4, for which the temperature dependence of the electrical conductivity has already been interpreted [9,14]. In the case of Fe_2CrO_4, when the number of Fe^{2+} is roughly equal to the number of Fe^{3+} ions ($Fe^{2+}/Fe^{3+} \approx 1$), the decreasing conductivity from 170°C (Fig. 2) can be regarded as being caused by the oxidation of Fe^{2+} ions at B sites. Pure magnetite, with a high initial conductivity (Fe^{2+} and Fe^{3+} ions initially present in equal amounts), always undergoes a large conductivity decrease during oxidation. In the case of Fe_2AlO_4, when the Fe^{2+} ions on B sites are initially more numerous than Fe^{3+} ions, the break at 150°C in the lg $\sigma = f(1/T)$ curve can be regarded as being due to Fe^{2+} ion oxidation, which favours electron exchange between Fe^{2+} and Fe^{3+} ions. The maximum of conductivity appears at about 192°C when the amounts of Fe^{2+} and Fe^{3+} ions on B sites are equivalent, and the conductivity then decreases. From these results, it appears that the first maximum of conductivity observed at 280°C for Fe_2MoO_4 in the absence of a break at lower temperatures strongly suggests that Fe^{2+} and Fe^{3+} ions on B sites in the initial spinel are nearly equal in concentration, thus supporting the distribution (1). The principal difference between the samples prepared from oxalate precursors and Fe_2MoO_4 is a somewhat larger crystallite size. The second maximum at about 405°C probably manifests the onset of oxidation of Mo^{3+} ions, which is further supported by the fact that there is an important mass gain accompanying this peak.

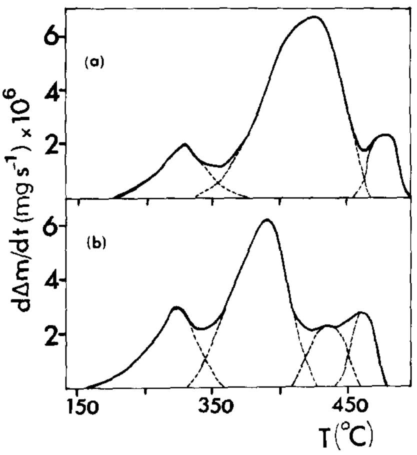

Fig. 3. DTG curves d $\Delta m/\mathrm{d}t = f(T)$ for Fe_2MoO_4 at 2.5°C min^{-1}, showing the effect of grinding time on oxidation behaviour: (a) 1 min; (b) 10 min.

Derivative thermogravimetry

The effect of the cation distribution between B and A sites and the influence of the grinding time were demonstrated directly by plotting d $\Delta m/\mathrm{d}t$ against T (m = mass; t = time), which for convenience is usually normalized to the starting mass (Fig. 3). For a grinding time of 1 min (chosen in order to have a good particle size, which enhances the reactivity, but at the same time to avoid mechanicochemical alterations of the sample), we observe after deconvolution three separate peaks (Fig. 3, curve a). The first peak at 310°C and the third peak at 615°C are due principally to the oxidation of Fe^{2+} ions on B sites and Fe^{2+} ions on A sites, respectively. These temperatures have been demonstrated elsewhere [9] from preliminary experiments during the oxidation of spinels containing solely an oxidizable cation (for example Fe^{2+}) located on only one site, i.e. Fe_3O_4 with Fe^{2+} ions on B sites and $FeCr_2O_4$ with Fe^{2+} ions on A sites. The second (intermediate) peak, which is obtained by deconvolution from the total curve, represents the oxidation of Mo^{3+} ions located in B sites. Indeed, the infrared spectra of samples oxidized above 400°C show an absorption band at 840 cm^{-1} assigned to Mo^{6+} ions.

The variation in intensity of each peak is indicative of the quantities of Fe^{2+}_{B}, Mo^{3+}_{B} and Fe^{2+}_{A} ions within the spinel [15]. In particular, a large rise in intensity in the temperature range $400 < T < 550$°C corresponds to the oxidation of Mo^{3+} to Mo^{6+} ions according to the reaction

$$2\,Mo^{3+} \rightarrow Mo^{6+} + \square$$

where □ denotes a cation vacancy.

TABLE 2

Dependence of S_t/S_0 ratio and oxidation temperature of each peak with grinding time

Grinding time	First peak $Fe^{2+}_B \rightarrow Fe^{3+}$		Second peak $Mo^{3+}_B \rightarrow Mo^{6+}$		Third peak $Mo^{4+}_B \rightarrow Mo^{6+}$		Fourth peak $Fe^{2+}_A \rightarrow Fe^{3+}$	
	S_t/S_0	T_{Ox} (°C)	S_t/S_0	T_{Ox} (°C)	S_t/S_0	T_{Ox} (°C)	S_t/S_0	T_{Ox} (°C)
1 min	0.55	308	1	490	0	–	0.45	609
10 min	0.85	295	0.75	431	0.25	525	0.40	572

The grinding time has a considerable effect on oxidation characteristics (Fig. 3, curve b); thus, for a sample ground for 10 min, the oxidation proceeded through four distinguishable steps with a variation in intensity and a shift of the peaks toward lower temperatures (Table 2). The additional peak observed at about 530°C can be regarded as being due to the presence of molybdenum in the tetravalent state generated by the grinding. Table 2 gives the S_t/S_0 ratio where S_t represents the area of each peak and S_0 is the area of the peak corresponding to pure magnetite. It can be seen that the concentration of Fe^{2+} ions on B sites is greater after a long grinding time but that the amount of Mo^{3+} ions has diminished to an appreciable degree as a result of the formation of Mo^{4+} ions. From these results the distribution of cations in Fe_2MoO_4 can be formulated as follows

$$(Fe^{2+}_{0.45}Fe^{3+}_{0.55})_A(Mo^{3+} + Fe^{2+}_{0.55}Fe^{3+}_{0.45})_B O_4^{2-} \qquad (3)$$

with $\beta = 0.45$ and $\alpha = 0$ for a grinding time of 1 min and

$$(Fe^{2+}_{0.40}Fe^{3+}_{0.60})_A(Mo^{3+}_{0.75}Mo^{4+}_{0.25}Fe^{2+}_{0.85}Fe^{3+}_{0.15})_B O_4^{2-} \qquad (4)$$

with $\beta = 0.40$ and $\alpha = 0.25$ for a grinding time of 10 min.

Characterization by XPS and IR spectroscopy. Evidence of Mo migration during oxidation

Figure 4 shows the X-ray photoelectron spectra of Fe_2MoO_4 in the Mo(3*d*) energy region for an initial sample ground for 10 min and for an oxidized sample. For the initial sample (curve a), two well resolved spectral lines at 235.8 and 232.9 eV were observed, indicating the presence of higher Mo–O oxidation states which are characteristic of Mo^{6+} [16] on the surface of Fe_2MoO_4. The third spectral line of lower intensity at 229.4 eV can be attributed to Mo^{4+} [16]. From these data, it is evident that the molybdenum initially in the trivalent state is not stable at the surface of Fe_2MoO_4 and that, moreover, a part of the molybdenum is present in the tetravalent state. After oxidation at 530°C (Fig. 4, curve b), we observe only two spectral lines at 235.9 and 233.1 eV, suggesting that the average oxidation state of Mo is close to 6 and that the Mo^{4+} ions have been oxidized.

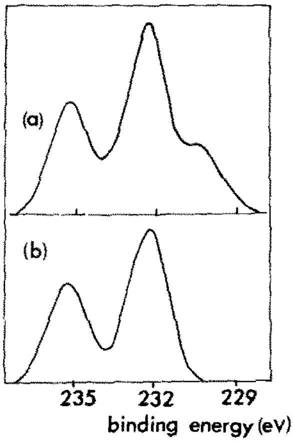

Fig. 4. XPS of the Mo 3*d* energy region in Fe_2MoO_4: (a) for an initial sample; (b) after oxidation at 550°C.

The FT-IR spectrum in the *n* Mo–O region for a ground unoxidized sample is reported in Fig. 5, together with the spectra of the samples after oxidation at different temperatures for 4 h. Before oxidation, and after oxidation at 285°C (curves a and b), no remarkable difference in the IR spectrum can be observed. In both cases a broad band centred at 726 cm^{-1} is present, together with some broad band absorption at lower frequency.

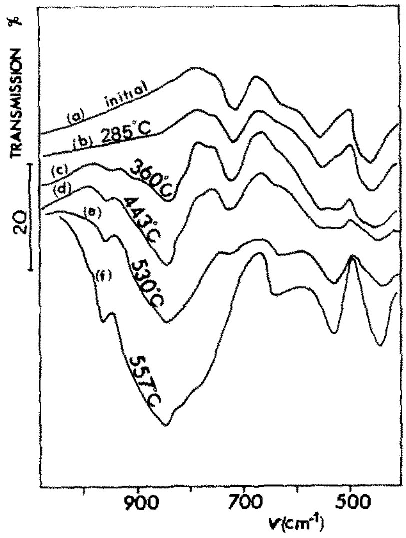

Fig. 5. Mo–O stretching frequencies for initial Fe_2MoO_4 and for Fe_2MoO_4 oxidized at different temperatures.

The high frequency band at 726 cm^{-1} of the spinel should be assigned to a vibration of octahedral groups according to the location of the highest valency cation, corresponding for a spinel to Mo^{4+} cations on B sites [17].

At higher oxidation temperatures (curves c, d, e), new bands appear near 840 and 960 cm^{-1}, indicating that these bands arise from MoO_4 tetrahedra. In Ag_2MoO_4, Na_2MoO_4 of spinel structure or most of the molybdates ($BaMoO_4$, $CaMoO_4$, $PbMoO_4$) in which the molybdenum is tetrahedrally coordinated by oxygens, the strong band at 840 cm^{-1} is also assigned to MoO_4 tetrahedra [18].

In addition, the absorption band at 726 cm^{-1} disappears around 530°C, which is associated with the oxidation of Mo^{4+} ions in B sites. For oxidation temperatures above 550°C, X-ray diffraction analysis indicates that the cation deficient spinel is converted into iron(III) molybdate $Fe_2(MoO_4)_3$ and α-Fe_2O_3. Following this transformation the IR spectrum presents two groups of well resolved bands which can be attributed to α-Fe_2O_3 in the 700–400 cm^{-1} region [19] and to $Fe_2(MoO_4)_3$ in the higher frequency absorption region. As shown in Fig. 5 (curve f), the high frequency absorption band at 840 cm^{-1} does not differ markedly from that observed before transformation, but is not unexpected in view of the structure of $Fe_2(MoO_4)_3$. Indeed, in this molybdate the oxygen atoms coordinate the iron atoms octahedrally and the molybdenum atoms tetrahedrally, and the octahedra share corners with the tetrahedra [20]. Thus, in all cases in which Mo(VI) is present, the absorption band at 840 cm^{-1} could be assigned to vibration of the tetrahedral MoO_4 group.

This assumption requires that the abstraction of three electrons from a Mo^{3+} ion to make a Mo^{6+} ion during oxidation in a cation deficient spinel induces a transfer of Mo^{6+} ions from the B sites to the A sites with a concomitant migration of Fe^{3+} ions from A to B sites. However, the kinetics for this migration are low relative to the kinetics of oxidation and depend on the length of time the system remains at the isothermal temperature or on the heating rate. Examination of the IR spectrum obtained for a sample heated in air at 370°C for 4 h (Fig. 6, curve a) and for a sample heated at 450°C for 30 min, or when the sample is heated at a constant rate of 2.5°C min^{-1} from 20 to 500°C (Fig. 6, curve b), shows that a long reaction time is favourable to a migration of Mo^{6+} ions on A sites. For a short reaction time, the band at 840 cm^{-1} is missing but the IR spectrum exhibits a series of bands near 600, 790, 860 and 920 cm^{-1} associated with the presence of Mo^{6+} ions located on B sites. This large number of bands depends on the fact that the MoO_6 octahedra are "elongated" with short and long to very long Mo–O distances, like α-$NiMoO_4$ [17].

From mass–charge balance considerations, and as it is also generally established that vacancies enter the lattice almost exclusively on B sites, it follows that the extended formula for a sample oxidized at 550°C can be

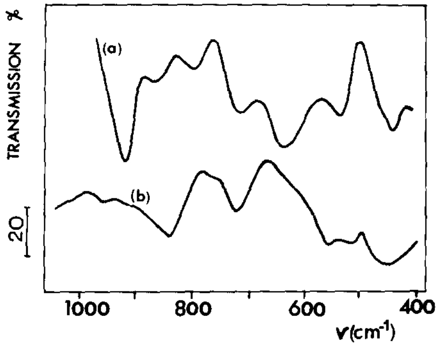

Fig. 6. Infrared spectra of cation deficient spinel: (a) Fe_2MoO_4 oxidized for 4 h at 370°C; (b) after slow heating to 500°C.

written as

$$\left(Fe^{2+}_{(72/y)}Fe^{3+}_{(99-100\delta/y)}Mo^{6+}_{(160\delta/y)}\right)_A\text{-}$$

$$\left(Mo^{3+}_{(160(1-\delta)/y)}Fe^{3+}_{(149+100\delta/y)}\square_{(3(11+60\delta)/y)}\right)_B O_4^{2-} \qquad (5)$$

where δ represents the content of Mo^{3+} oxidized at 550°C and $y = 171 + 60\delta$. For $\delta = 0.72$, the number of vacancies approaches 0.75 per "molecule" and is far larger than that obtained in γ-Fe_2O_3 ($\square = 0.33$) or in γ-Fe_2TiO_5 ($\square = 0.56$) [10].

CONCLUSIONS

In the present work, we have shown that Fe_2MoO_4 prepared at high temperature and ground is highly reactive towards oxygen and could be oxidized below 550°C to a cation deficient spinel with a larger vacancy content than that found up to now for this type of mixed oxide.

The electrical conductivity data for Fe_2MoO_4 are in agreement with the relative availability for oxidation of Fe^{2+} and Mo^{3+} ions, and confirm an electron hopping between Fe^{2+} and Fe^{3+} ions. The valence transfer may occur at octahedral sites as well as tetrahedral sites with a fraction of the Mo atoms in electronic transport.

Derivative thermogravimetry shows a three or four stage oxidation process depending on the duration of grinding when the oxidation temperature is related to the distribution of Fe^{2+}, Mo^{3+} and Mo^{4+} ions on B sites and Fe^{2+} ions on A sites. A quantitative analysis of cations from the determination of oxidation peak areas based on this discrepancy of reactivity permits us to propose a cationic distribution for the cation deficient spinel.

Besides the cationic distribution determination, some other features of the change in valency state of ions and of the thermal stability during oxidation have been determined from the spectroscopic behaviour. In particular, the presence of Mo^{4+} ions on B sites has been established for ground samples and the cationic distribution in a slowly oxidized spinel should take into account the migration of Mo^{6+} ions on A sites, which is responsible for the infrared band observed at 840 cm^{-1}. Above 550°C, we have a crystallographic transformation of the spinel structure into α-Fe_2O_3 and $Fe_2(MoO_4)_3$. In this latter compound, in which the oxygen atoms also coordinate the molybdenum atoms tetrahedrally, the strong absorption band observed at 840°C confirms that the Mo(VI) is tetrahedrally coordinated by oxygen in the cation deficient spinel.

REFERENCES

1 M. Abe, M. Kawachi and S. Nomura, J. Phys. Soc. Jpn., 31 (1971) 940.
2 M. Abe, M. Kawachi and S. Nomura, J. Phys. Soc. Jpn., 34 (1973) 565.
3 J. Ghose, N.N. Greenwood, A.C. Halam and D.A. Read, J. Solid State Chem., 11 (1974) 239.
4 E.J.W. Verwey and P.W. Hayman, Physica, 8 (1941) 979.
5 B. Gillot, M. El Guendouzi, A. Rousset and P. Tailhades, J. Mater Sci., 21 (1986) 2926.
6 B. Gillot, M. Kharroubi, R. Metz, R. Legros and A. Rousset, Phys. Status Solidi A, 123 (1991) 125.
7 M. Gupta, S. Kanetkar, S. Date, A. Nigakevar and A. Sinha, J. Phys. C, 12 (1979) 2411.
8 A. Ramdani, C. Gleitzer, G. Gavolle, A.K. Cheetham and J.B. Goodenough, J. Solid State Chem., 60 (1985) 269.
9 B. Gillot, F. Jemmali, F. Chassagneux, C. Salvaing and A. Rousset, J. Solid State Chem., 45 (1982) 317.
10 B. Gillot, F. Jemmali, L. Clerc and A. Rousset, React. Solids, 2 (1986) 95.
11 B. Gillot, J.F. Ferriot and A. Rousset, J. Phys. Chem. Solids, 37 (1976) 857.
12 P. Poix, F. Basile and C. Djega-Mariadasson, Ann. Chim. (Paris), 10 (1971) 159.
13 S.E. Dorris and T.O. Mason, J. Am. Ceram. Soc., 71 (1988) 379.
14 B. Gillot, F. Bouton, F. Chassagneux and A. Rousset, Phys. Status Solidi A, 50 (1978) 109.
15 M. Laarj, I. Pignone, M. Guendouzi, P. Tailhades, A. Rousset and B. Gillot, Thermochim. Acta, 152 (1989) 187.
16 A. Katrib, A. Stanislaus, M. Absi-Halabi and K. Al Dolama, in D.L. Trimm et al. (Ed.), Catalysis in Petroleum Refining, Elsevier, Amsterdam, 1989.
17 P. Tarte, A. Rulmont, M. Liegeois-Duyckaers, R. Cahay and J.M. Winand, Solid State Ionics, 42 (1990) 177.
18 G.M. Clare and W.P. Doyle, Spectrochim. Acta, 22 (1966) 1441.
19 B. Gillot, R.M. Benloucif and A. Rousset, J. Solid State Chem., 39 (1981) 329.
20 P.D. Battle, A.K. Cheetham, G.L. Long and G. Longworth, Inorg. Chem., 21 (1982) 4223.